Tropospheric Double Jets, Meridional Cells, and Eddies: A Case Study and Idealized Simulations

ISABELLA BORDI

Department of Physics, University of Rome "La Sapienza," Rome, Italy

KLAUS FRAEDRICH AND FRANK LUNKEIT

Meteorologisches Institut, Universität Hamburg, Hamburg, Germany

ALFONSO SUTERA

Department of Physics, University of Rome "La Sapienza," Rome, Italy

(Manuscript received 30 June 2006, in final form 2 January 2007)

ABSTRACT

The observed low-frequency variability of the zonally averaged atmospheric circulation in the winter hemisphere is found to be amenable to an interpretation where the subtropical jet is flanked by a secondary midlatitude one. Observations also suggest that the link between the stratosphere and the troposphere modulates the variability of the tropospheric double-jet structure. Moreover, the summer hemisphere is characterized by a strong midlatitude jet sided by an intermittent subtropical one and easterly winds in the stratosphere. This work addresses the question about the role of eddies in generating and maintaining these key features of the general circulation by means of a simplified general circulation model. Model solutions for different parameter settings and external radiative forcings in the stratosphere are studied with and without eddies active on the system. The following main findings are noted. 1) Eddy dynamics alone, through the baroclinic instability processes in an atmosphere subjected to radiative forcing and dissipation, may account for the observed meridional variance of the tropospheric jets. 2) The Hadley cell can extend to the pole overlying the Ferrel cell, a feature supported by observations in the summer hemisphere. 3) The meridional temperature gradient reversal in the summer stratosphere contributes to the observed low-frequency variability introducing an intermittent formation of a subtropical jet and the occurrence of easterlies in the tropical stratosphere. 4) Poleward propagation of the zonal wind anomaly is, when it occurs, related to the activity of synoptic eddies.

---

1. Introduction

The most prominent feature of the general circulation is the presence of a mean westerly jet at the tropopause level in the Tropics. Moreover, when we consider, for example, the observed Northern Hemisphere zonally averaged zonal wind standard deviation, we find two relative maxima located in the subtropics and midlatitudes. Thus, a central problem is the finding of the physical mechanisms that originate and maintain these observed features. Since the works of Rossby and

Starr (1949) and Palmén (1949), the issue has been whether the climatological jet is created and maintained by the transport properties of the eddies, generated by the baroclinic instability of the thermal wind, or by the combined effects of the imposed radiative differential heating and the Coriolis torque, as the angular momentum conservation principle suggests. A difficulty with the latter approach is that the meridional velocity, produced by the buoyancy forces associated with the differential heating, is so small that the time involved in the cell is of the order of 100 days. In such a slow motion, the Coriolis torque must be balanced by dissipation of the zonal velocity, so that the determination of the diffusion coefficient becomes the key to the solution. On the other hand, the eddy-driven case is strongly related to the nature of the eddy transports.

Corresponding author address: Dr. Alfonso Sutera, Department of Physics, University of Rome "La Sapienza," I-00185 Rome, Italy.
E-mail: alfonso.sutera@roma1.infn.it

These transports are the outcome of complex nonlinear processes that involve both the zonal mean fields and the eddies. In absence of an accepted parameterization, these processes can be only simulated.

Observations, however, may be of some help in suggesting the origin of the jet(s). Following the papers of Rossby and Willet (1948) and Namias (1950), it has been recognized that the jet(s) axis occasionally undergoes a vacillation, so that its position is not always located around the climatological mean. More recently, Koo et al. (2002, see also references therein) confirmed these early observations by showing a bimodal distribution of the Southern Hemisphere jet axis position, when the mean zonal wind variance is projected onto the first two principal components.

On the theoretical side, Lorenz (1963), also motivated by the experimental results found in the annulus, proposed a simple model of the jet vacillation using a quasigeostrophic model in the β plane. In that paper the author discussed how the eddy momentum fluxes, associated to baroclinic waves, may lead to a vacillating jet in the troposphere and noticed that the nature of wave breaking is cyclonic northward of the jet axis and anticyclonic on its southern flank. Using primitive equation models forced by a Newtonian cooling, a similar behavior was found (just to mention a few authors) by Hendon and Hartmann (1985), James et al. (1994), Akahori and Yoden (1997), Caballero et al. (2001), and more recently by Koo et al. (2005, manuscript submitted to *Quart. J. Roy. Meteor. Soc.*).

On the other hand, Hunt (1978), following the theoretical analysis of Matsuno (1970) and Dickinson (1968), reported that stratosphere–troposphere coupling could induce a similar vacillation. It was associated to the pressure work exerted by baroclinic waves and by vertical propagation of stationary waves into the stratosphere.

In recent years, the interest in the stratosphere–troposphere interaction has also increased because the observed ozone layer variations may be related to anthropogenic pollutants. Since, in addition to biological effects, ozone variations may have impacts on climate, several works have been devoted to the study of the influence of the stratosphere on the tropospheric circulation (see, e.g., Boville 1984; Kushner and Polvani 2004; Wittman et al. 2004). Albeit Hartmann et al. (2000) have recently reported progresses in the understanding of this process, the precise nature of this interaction is yet poorly qualified. Theoretical reasoning, such as the one proposed by Lindzen (1993) and discussed in Bordi et al. (2002, 2004), have outlined a possible stratosphere–troposphere interaction through the modification of the baroclinic instability property of an atmosphere without a rigid lid at the tropopause. This mechanism may feed back on to the atmospheric general circulation through the eddy heat and momentum fluxes (Lorenz 1967). Along this line, a cursory look to the zonally averaged zonal momentum equation clearly shows that, in absence of internal dissipation, the advection of the total zonal mean vorticity by the zonal mean meridional circulation should be balanced against surface friction by the eddy momentum fluxes. Thus, it appears that the maintenance of the jet(s) variability may be strongly influenced by complex modifications of baroclinic waves when a coupling between the stratosphere and troposphere is considered.

In the scientific community there is a general consensus on the different mechanisms generating the subtropical and midlatitude jets. The former is thought to be generated by angular momentum transports of the Hadley circulation (Held and Hou 1980), while the latter is an eddy-driven jet and results from eddy momentum flux convergence of baroclinic waves (Held 1975; Panetta 1993). Recently, this point of view, in particular the origin of the subtropical jet, has been a matter of further investigations. Model simulations (Caballero et al. 2001; Walker and Schneider 2006; Schneider 2006), in fact, suggest that eddies might also have an important role in establishing the subtropical jet.

In the present paper we will study the role of synoptic eddies in generating and maintaining the main features of the zonally symmetric circulation following Charney's (1959, 1973) approach by

1) finding observational evidence for the existence of multiple jets in both hemispheres and their intermittent nature represented by the observed (meridional) variance structure of the tropospheric jets;
2) trying to connect these features to the stratospheric circulation by means of solutions of simple primitive equations forced by an equatorially symmetric Newtonian cooling, in a dry atmosphere with a weak stratospheric jet; and
3) connecting the antisymmetric forcing in the stratosphere with the intermittent nature of the subtropical jet in the Southern Hemisphere summer.

In particular, we wish to propose a different interpretation of the zonally averaged flow vacillation, namely we suggest that two distinct tropospheric jets may coexist at the same time (in the same hemisphere) and that the zonal mean flow in the stratosphere plays a significant role in determining this behavior.

The paper is structured as follows. First, we will show hints of the validity of this proposal by considering atmospheric data for a few cases (section 2). Next, we will use a primitive equations model forced by Newtonian
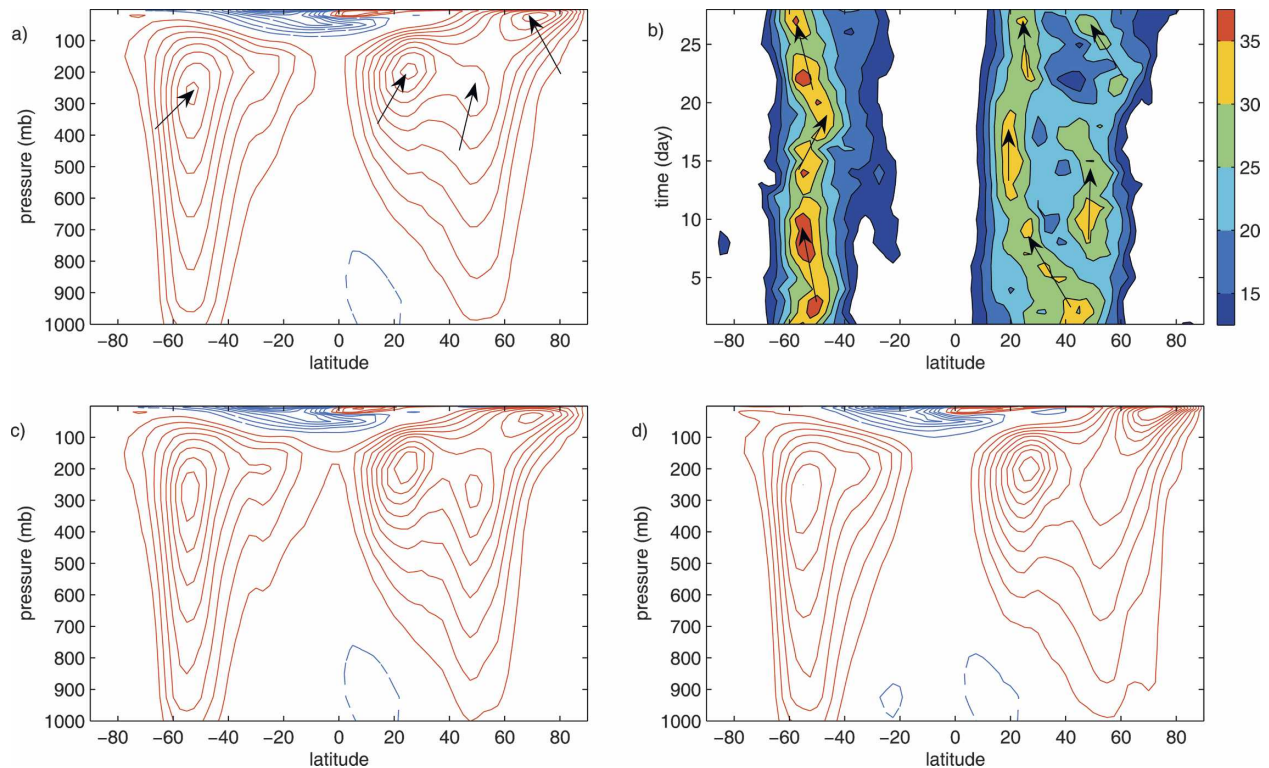
FIG. 1. Observations of February 1990: (a) latitude–height (pressure) cross section of the monthly mean zonal wind (arrows pointing to the relative maxima), (b) time evolution (Hovmoeller diagram) of the zonal mean zonal wind at 300 mb (arrows pointing to the jets' locations), and time-averaged zonal mean zonal wind for days (c) 7–16 and (d) 20–28. Units are m s^{-1}. (a), (c), (d) Contours are every 4 m s^{-1} and the zero line is excluded; red lines denote positive values and blue lines negative values.

cooling. To isolate the role of the baroclinic instability in the formation of multiple tropospheric jets, we intentionally neglect any form of convection, land–sea contrast, and orography in the model atmosphere. In the troposphere, friction or diffusion is only present at the earth surface except for the small hyperdiffusion required for numerical stability. Therefore, the zonal mean circulation can be ascribed only to the action of the eddies and/or to the stratosphere (section 3). This model, for given parameter settings and different structures of the external radiative forcing in the stratosphere, produces two jet cores, one in the subtropics and one in the midlatitudes, maintained by eddy dynamics alone (section 4). Conclusions are presented in section 5.

2. Double jets observed in the troposphere: A case study

We illustrate the low-frequency variability of the observed jet streams by considering a sample month of the 40-yr European Centre for Medium-Range Weather Forecasts (ECMWF) Re-Analysis (ERA-40) dataset (horizontal resolution of 2.5° × 2.5°, 23 pressure levels from 1000 to 1 mb).

a. Time mean and variability of zonal flow

As an example, the behavior of February 1990 is analyzed. Figure 1a shows the monthly mean zonally averaged zonal wind as a function of latitude and pressure. The added arrows indicate the position of the main jet cores. In the Northern Hemisphere (winter) three jets are present: two of them are below the tropopause, while the third one is well within the stratosphere. In the Southern Hemisphere (summer), there is a well-defined jet located at around 50°S, while farther north there is a hint of a secondary subtropical jet maximum. Easterlies characterize the stratosphere from the tropical region to about 60°S.

The novelty of Fig. 1a lies in the appearance of two well-defined jets in the Northern Hemisphere (winter) troposphere, both reaching their maximum speed at the local tropopause level. The question is whether this feature denotes a jet axis vacillation or an actual coexistence of the two jet cores. To distinguish between these two alternatives, the easiest way is to consider the time

behavior of the zonally averaged zonal wind at a given pressure level, say 300 mb, as shown in Fig. 1b. A few arrows have been added to help the reader to locate the jets and their meridional wandering. From an inspection of both figure panels, one can see a main midlatitude jet core, flanked by a weaker subtropical one, is present in the summer Southern Hemisphere while, occasionally, two jets (also vacillating) coexist in the winter Northern Hemisphere. In the stratosphere, instead, there is only a winter polar jet while, elsewhere, a weak westerly or a sustained easterly jet prevails. This behavior is quite commonly observed, including months when the mean map is not as revealing as it is in this particular month. Moreover, Fig. 1b suggests separately considering the time averages over the period from days 7 to 16 and from days 20 to 28. The zonally averaged zonal wind for these two periods is presented in Figs. 1c,d. In the Northern Hemisphere, both figures show two coexisting tropospheric jets:

(i) In the first period (days 7–16), the midlatitude jet is cut off from the stratospheric polar one, which seems to be weaker than its monthly mean (about 5 m s^{-1} less).

(ii) In the second time period (days 20–28), there is a connection between the midlatitude tropospheric jet and the polar stratospheric one whose strength has increased sensibly above the monthly mean (about 8 m s^{-1} greater).

That is, there are at least two diverse mechanisms leading to a double-jet formation, both involving the stratosphere. An analysis of the eddy field provides the possible link between the troposphere and stratosphere.

b. Eddy fluxes

The zonally averaged eddy meridional momentum and heat fluxes (i.e., the simple correlation between the proper fields) for all three time periods (the entire month and the first and second periods) are shown in Fig. 2. Let us focus on the Northern (winter) Hemisphere.

(i) The midlatitude jet depicted in Fig. 1c (first period) is accompanied by a strong reversal of the meridional eddy momentum flux as shown by Fig. 2b, whereas in the second period the meridional momentum flux (Fig. 2c) compares well with that for the monthly mean (Fig. 2a). Thus, the set of Figs. 1c,d and Figs. 2b,c suggests that the days 20–28 event relates to the monthly averaged tropospheric

wave–mean flow interaction, while the other period does not.

(ii) Also the eddy heat fluxes show for the first period a change of sign in the Northern Hemisphere at the tropopause level (see contour lines in Fig. 2b). The heat fluxes of days 20–28 (Fig. 2c), instead, are similar to those of the monthly mean, indicating that in the second period the tropospheric transient eddies are not behaving anomalously.

Thus, the overall picture suggests that, for the first time interval (days 7–16), the eddy forcing alone is acting anomalously by reinforcing and creating enough divergence to maintain a midlatitude secondary jet. Moreover, in this month the latitudinal jet vacillation appears to be a feature of only secondary importance. Furthermore, the Southern Hemisphere (summer) is also characterized by a reversal of the meridional eddy momentum fluxes, which are stronger during the second period (days 20–28) associated with an intensification of the subtropical jet and strong easterlies at lower levels.

In assessing the role of the eddies in establishing these behaviors, we use the component of the zonal momentum budget described by Eliassen–Palm (E–P) fluxes (Eliassen and Palm 1961) as defined in Edmon et al. (1980). Specifically, if ω and θ are the pressure velocity and the potential temperature, respectively, and in view of large static stability of the atmosphere (Peixoto and Oort 1992), we may set

$$\frac{\partial [\omega][\theta]}{\partial p} \approx [\omega] \frac{\partial [\theta]}{\partial p}, \qquad (1)$$

where p is the pressure and $[.] = \int (.) \, d\lambda$. The E–P vector $\mathbf{F}$ in the (ϕ–p) plane, with ϕ the latitude, is computed as

$$\mathbf{F} = \frac{2\pi R^2 \cos\phi}{g} \left(\frac{1}{R} F^\phi, F^p \right), \quad \text{with}$$

$$F^\phi = -R \cos\phi [u'v'] \quad \text{and}$$

$$F^p = fR \cos\phi [v'\theta'] \bigg/ \frac{\partial [\theta]}{\partial p}. \qquad (2)$$

Here R is the radius of the earth, f is the Coriolis parameter, primes denote the departure from the zonal average, and the remaining variables have the usual meaning.

To obtain a graphical representation of the E–P flux $\mathbf{F}$ and its divergence, the procedures given by Edmon et al. (1980) are followed. Instead of the divergence of $\mathbf{F}$, the divergence weighted by the mass of an annular ring $d\phi \, dp$ is used:
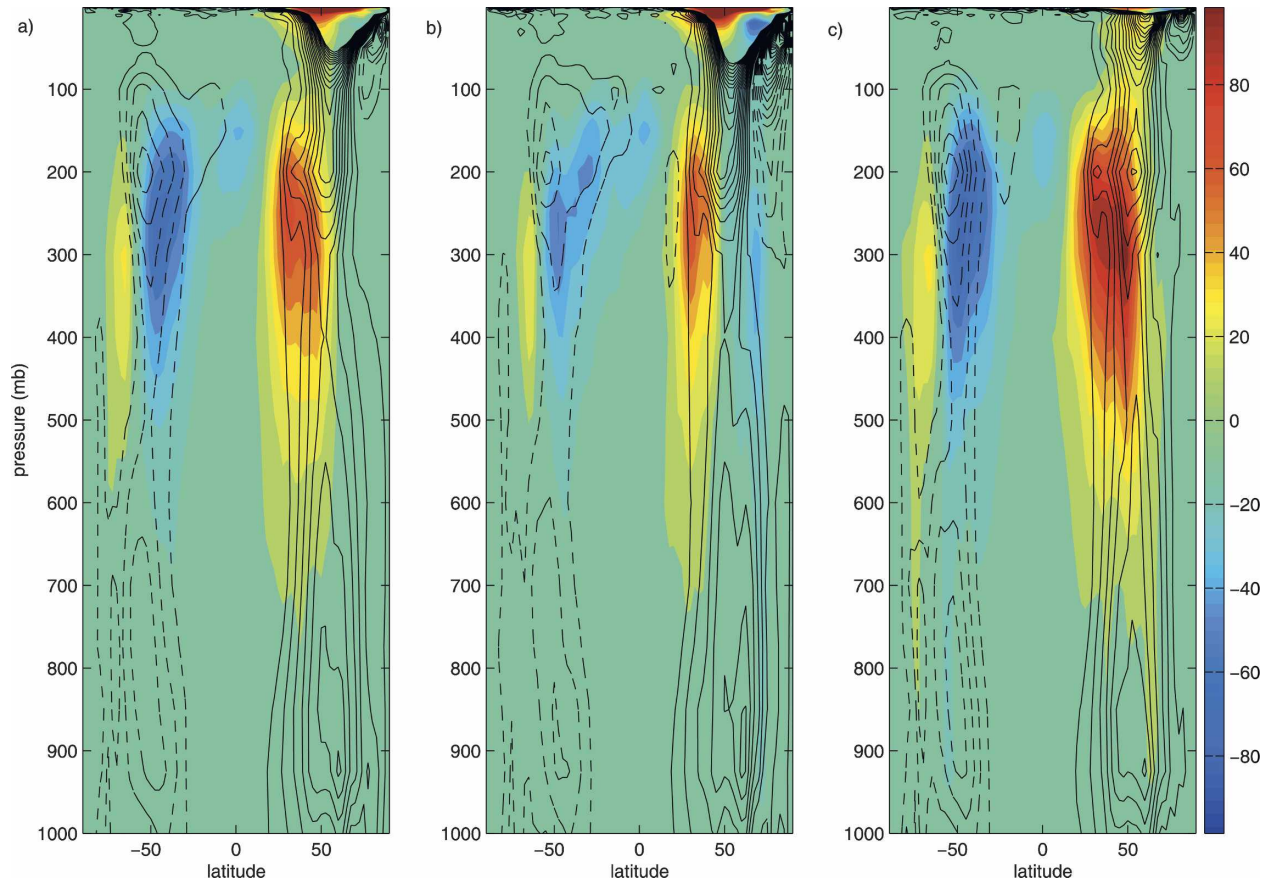
FIG. 2. Observations of February 1990: mean meridional eddy momentum flux ($u'v'$ correlation, contour shaded) and mean meridional eddy heat flux ($v'\theta'$ correlation, contour lines) for (a) monthly mean, and for days (b) 7–16 and (c) 20–28. Units are m^2 s^{-2} for $u'v'$ and m s^{-1} K for $v'\theta'$. Contour lines are every 5 m s^{-1} K and the zero line is excluded; solid lines denote positive values, dashed lines negative values.

$$\mathrm{div}(\hat{\mathbf{F}}) = \frac{\partial \hat{F}^\phi}{\partial \phi} + \frac{\partial \hat{F}^p}{\partial p}, \qquad (3)$$

where

$$\hat{F}^\phi = \frac{2\pi R}{g}\cos\phi F^\phi \quad \text{and} \quad \hat{F}^p = \frac{2\pi R^2}{g}\cos\phi F^p. \quad (4)$$

Figures 3a–c present the E–P flux vectors $\hat{\mathbf{F}}$ and its divergence for the monthly mean, and during days 7–16 and 20–28, respectively. As anticipated, Fig. 3b (first period) shows, in the Northern Hemisphere, a peculiar difference from the second period: at high-tropospheric layers in midlatitudes the direction of $\hat{\mathbf{F}}$ points poleward. This anomalous action of the eddies also involves the stratosphere, where a weaker, than the monthly mean, polar jet occurs. Moreover, in correspondence to the split of the E–P vectors, a positive divergence around 250 mb is noticeable, suggesting that the eddies play a crucial role in creating the double-jet structure. Following the usual interpretation of the E–P vectors, in the first period Rossby waves, generated by the baro-

clinic instability, propagate both equatorward and poleward out of the main jets' axes. Note also that the convergence of the eddy momentum fluxes in the subtropics and midlatitudes, implies an anticyclonic breaking of the eddies near the equator and a cyclonic one near the poles. The other maps, instead, depict the usually observed convergence of $\hat{\mathbf{F}}$ toward the equator. This suggests that the eddy fluxes are the main contributors to the anomalous double-jet configuration found during days 7–16. Moreover, observations for February 1990 seem to support the hypothesis that the eddies play a crucial role in also establishing the subtropical jet: the local Rossby number ($R_0 = -\bar{\zeta}/f$ as in Schneider 2006), which should be around 1 for the Held and Hou solution, is less than 0.5 in the upper branch of the Hadley cell and a meridional gradient of angular momentum is noticeable everywhere (excluding regions near the equator).

If we suppose that the momentum budget only reduces to (3), then the data analysis above poses the question whether a thermally forced atmosphere may
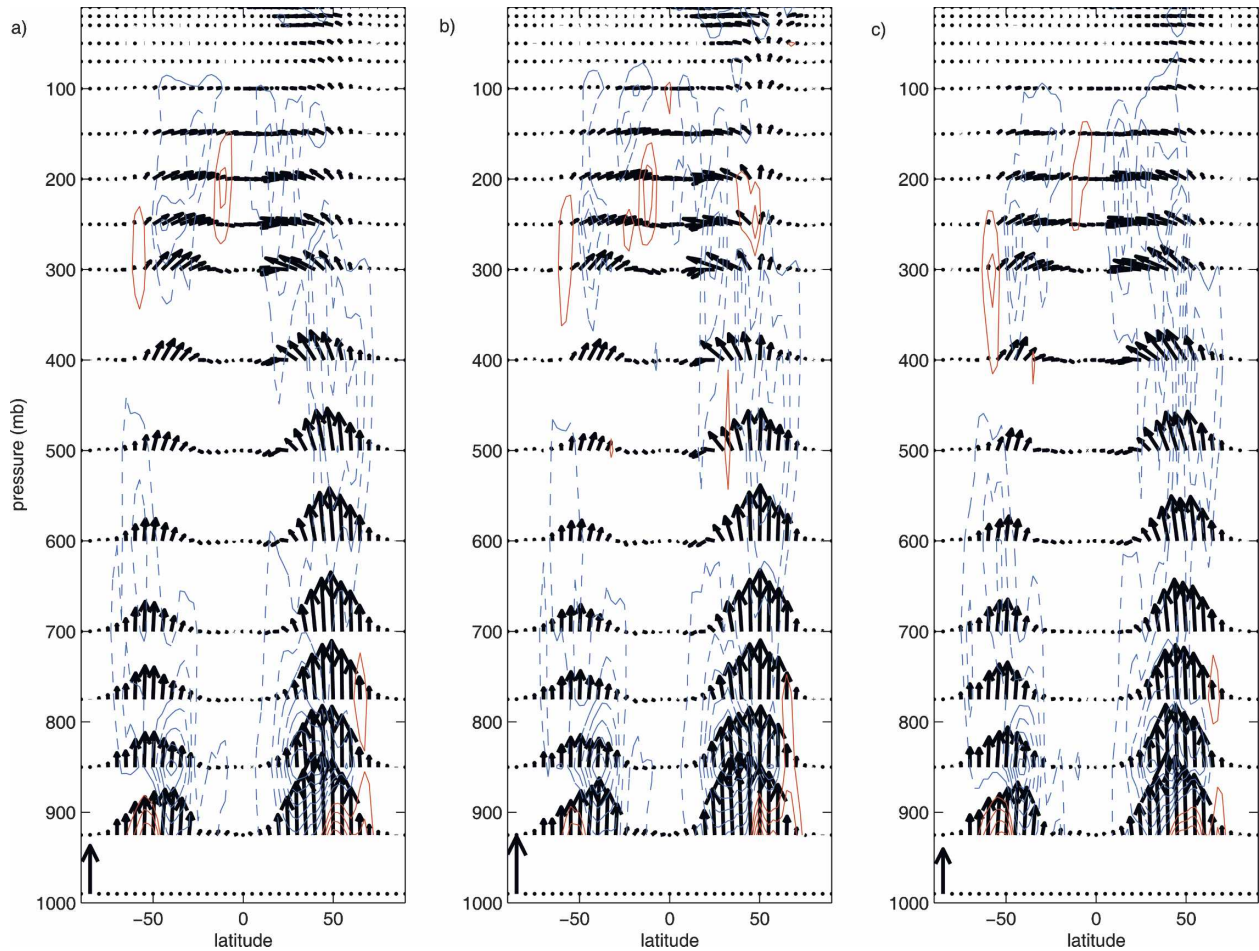
FIG. 3. Observations of February 1990: E–P flux vectors (arrows) and flux divergence (isolines) for (a) monthly mean, and for days (b) 7–16 and (c) 20–28. Contours for the divergence are every 2×10^{15} m^3 and the zero line is excluded; solid red lines denote positive values, dashed blue lines negative values. The vertical arrow scale for $\hat{F}^p$ (4.02×10^{15} m^3 mb) is indicated in the bottom left of each panel; the scale for the horizontal component $\hat{F}^\phi$ in m^3 is equal to the scale for $\hat{F}^p$ but divided by 804 mb.

develop a circulation consistent with these observations in virtue of the transient eddy forcing alone as in Lorenz (1963). Moreover, there is a hint that the strength of the zonal mean zonal wind in the stratosphere plays a role in determining the tropospheric circulation as in Hunt (1978). This will be the subject of section 3 using an idealized general circulation modeling approach.

3. Model and experiments

In the present paper numerical solutions are found by using the simplified GCM Portable University Model of the Atmosphere (PUMA; Fraedrich et al. 1998; available online at http://www.mi.uni-hamburg.de/puma). PUMA is a global spectral model (Hoskins and Simmons 1975; James and Gray 1986) that solves the primitive equations on sigma levels. The diabatic

and dissipative processes are represented through the Newtonian cooling and the Rayleigh friction, respectively (Held and Suarez 1994). PUMA has been used to simulate other features of the atmospheric circulation such as, for example, the storm track variability (see Frisius et al. 1998; Fraedrich et al. 2005). The model is run at T21 resolution with 20 equally spaced σ levels. The T21 horizontal resolution is set to follow James et al. (1994). The 20 vertical levels are an attempt to have enough resolution in the stratosphere, with a reasonable computational burden.

a. Parameter settings

In the present study we offer a view of the general circulation as a forced response to a given steady external forcing (of a radiative nature). Therefore, its specification is more than a detail. First, we consider the same forcing as Akahori and Yoden (1997) as de-

scribed in their Table 1. The reason for this choice is simply that the forcing in the above-mentioned paper is clearly specified at the same number of vertical levels as we have. Their model's forcing is given on variable vertical resolution, which is interpolated to our σ levels. The PUMA settings for the zonally symmetric aqua planet–type circulation are as follows.

1) NEWTONIAN COOLING

At each time step the model temperature is relaxed toward a prescribed restoration temperature field T^*, which, as in Akahori and Yoden (1997), describes hemispherically symmetric or equinox conditions:

$$T^*(\phi, \sigma) = T_0(\sigma) + \frac{\Delta T(\sigma)}{2}\left(\cos 2\phi - \frac{1}{3}\right), \qquad (5)$$

where $T_0(\sigma)$ is the global mean temperature at each level and $\Delta T(\sigma)$ is the pole-to-equator temperature difference. The relaxation time for the Newtonian forcing, τ_N, is 15 days for all levels, with the exception of the uppermost level, where it is set to 7.6 days. The restoration temperature may be interpreted as a sort of radiative equilibrium temperature and it is assumed to be identical in both hemispheres as we were representing ideal equinox conditions.

In the stratosphere we also consider a nonsymmetric (with respect to the equator) radiative forcing with a reversed meridional temperature gradient in the Southern Hemisphere, such that

$$T^*(\phi, \sigma) = T_0(\sigma) - \Delta T(\sigma)\sin\phi \quad \text{for} \quad \sigma < \sigma_T, \qquad (6)$$

with σ_T being the tropopause sigma level. This produces a reversed equator-to-pole temperature gradient in the model Southern Hemisphere stratosphere, while, in the Northern Hemisphere, it remains of the same sign as it is in the troposphere.

2) HORIZONTAL DIFFUSION

A hyperdiffusion ($K\nabla^8$, with K as the diffusion coefficient) is applied to temperature, divergence, and vorticity to prevent accumulation of enstrophy at the shortest scales and to preserve numerical stability.

3) RAYLEIGH FRICTION

The Rayleigh friction may act on each model level. Divergence and vorticity are damped with a time scale (TFRC) of 0.5 days at the lowermost level and, when explicitly mentioned, at a few uppermost levels. In particular, when we consider a reversal of the meridional temperature gradient in the stratosphere, we omit the Rayleigh friction everywhere but at the surface.

4) INITIALIZATION

The model starts either from a restart file or with an atmosphere at rest. We use the default that makes the initial state a motionless atmosphere with stable stratification. At the start, the divergence and the relative vorticity are set to zero and the departure from the restoration temperature is initialized as a horizontally constant field, while its vertical structure is adopted from the restoration temperature that is stably stratified. Initialization of the model can be prescribed as follows: if all modes are set to zero, the model will run without eddies; if a random white noise perturbation is generated, which is symmetric or nonsymmetric with respect to the equator, eddies are initialized.

b. Experimental design and diagnostic tools: Modifying the stratosphere

The model experiments described in the following (see Table 1) demonstrate the double-jet structure, the effect of eddies, and the relevance of the stratosphere in generating the features observed.

1) EXPERIMENTS

The PUMA reference experiment (C-1a) is characterized by a global mean temperature profile with the tropopause height at 275 mb and it includes all other constituents described in section 3a. This reference experiment may be compared with the Akahori and Yoden (1997) model experiment where the tropopause height was at 125 mb (C-0). Apart from hyperdiffusion, there is no internal dissipation (e.g., vertical diffusion) in the troposphere, so that, in absence of eddies, the atmospheric model solution will converge strictly to a thermal wind balance with zero meridional velocity and westerly zonal wind at the equator. As it is known, the symmetric solution of this setup does not violate Hide's theorem (see Schneider and Lindzen 1977; Held and Hou 1980; Lindzen 1990; Fang and Tung 1994). Moreover, any resulting mean meridional circulation may be entirely ascribed to the eddy dynamics, which is responding to the Newtonian thermal forcing. To mimic the observations the following modifications are made.

1) The first modification (C-1b) of the reference setup is the introduction of Rayleigh friction at high levels above the radiative tropopause. The use of Rayleigh friction may be interpreted as a parameterization of the gravity wave drag in the upper model layers. It also acts as a sponge to prevent spurious wave reflection from the upper boundary (see, e.g., Norton 2003; Scott and Polvani 2004). For our purpose the Rayleigh friction has the scope to let the jet decrease
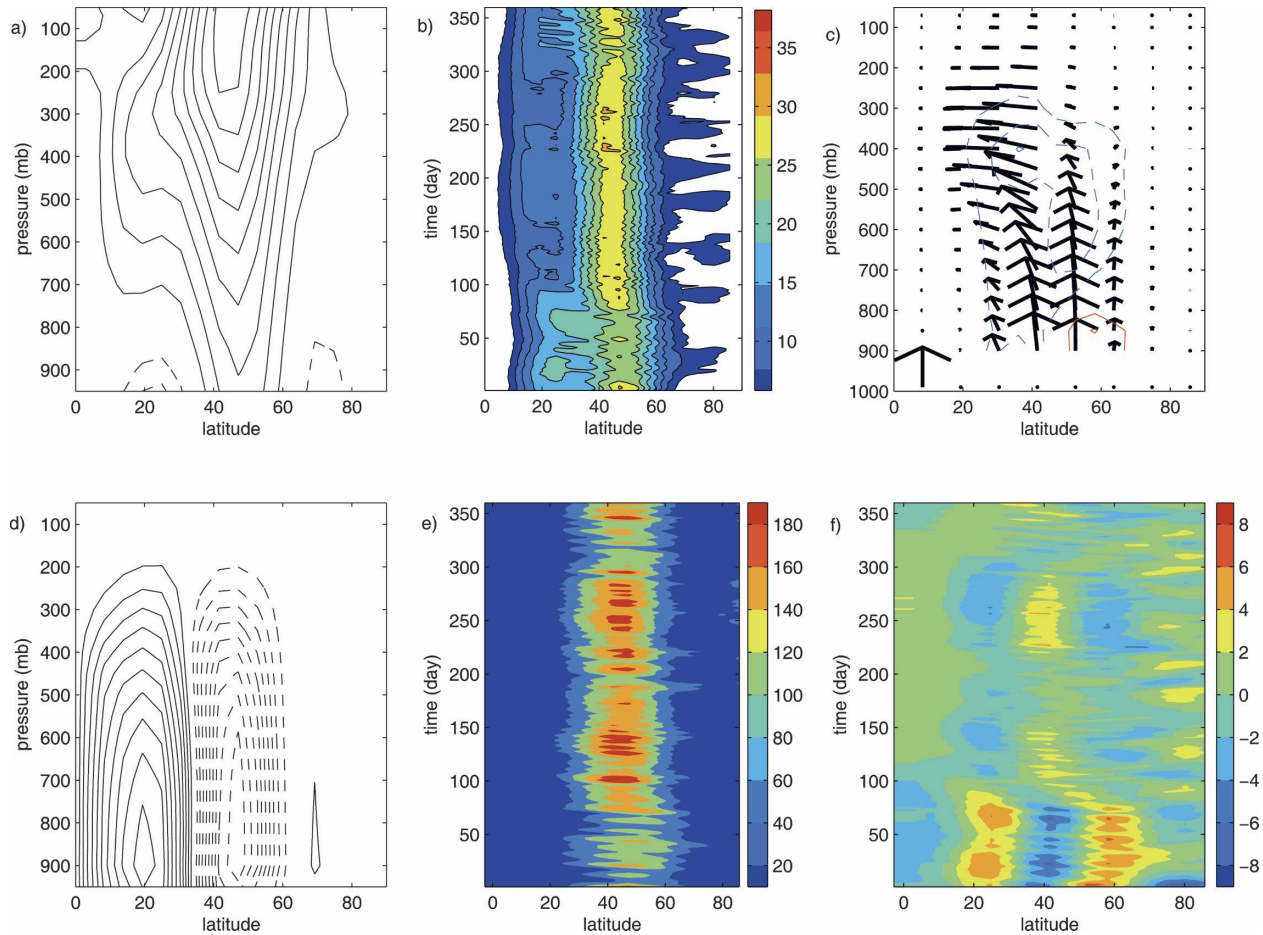
TABLE 1. Experimental setup for PUMA: the global mean restoration temperature $T_0(\sigma)$, the pole-to-equator temperature difference $\Delta T(\sigma)$, and the Rayleigh friction damping time scale TFRC. Remarks are in the last column.

Case	$T_0(\sigma)$ (K) top to bottom	$\Delta T(\sigma)$ (K) top to bottom	TFRC(σ) (day^{-1}) top to bottom	Remarks
C-0	224.14, 213.91, 211.36, 212.95, 217.56, 224.07, 231.24, 237.73, 243.54, 248.87, 253.41, 257.83, 261.72, 265.60, 268.96, 272.33, 275.36, 278.34, 281.06, 283.74	0.00, 0.00, 2.00, 9.19, 19.13, 28.26, 34.91, 40.37, 45.10, 49.19, 52.05, 54.69, 56.20, 57.70, 58.31, 58.91, 59.26, 59.56, 59.76, 59.94	0.0, 0.0, 0.0, 0.0, 0.0, 0.0, 0.0, 0.0, 0.0, 0.0, 0.0, 0.0, 0.0, 0.0, 0.0, 0.0, 0.0, 0.0, 0.0, 0.5	Akahori and Yoden (1997): Forcing temperature profile with high tropopause
C-1a	265.14, 254.91, 246.36, 240.95, 237.56, 234.65, 235.24, 237.73, 243.54, 248.87, 253.41, 257.83, 261.72, 265.60, 268.96, 272.33, 275.36, 278.34, 281.06, 283.74	0.00, 0.00, 0.00, 0.00, 0.00, 28.26, 34.91, 40.37, 45.10, 49.19, 52.05, 54.69, 56.20, 57.70, 58.31, 58.91, 59.26, 59.56, 59.76, 59.94	0.0, 0.0, 0.0, 0.0, 0.0, 0.0, 0.0, 0.0, 0.0, 0.0, 0.0, 0.0, 0.0, 0.0, 0.0, 0.0, 0.0, 0.0, 0.0, 0.5	Reference expt: Forcing temperature profile with the lower tropopause
C-1b	As for C-1a	As for C-1a	0.2, 0.2, 0.0, 0.0, 0.0, 0.0, 0.0, 0.0, 0.0, 0.0, 0.0, 0.0, 0.0, 0.0, 0.0, 0.0, 0.0, 0.0, 0.0, 0.5	Reference expt: Forcing temperature profile with Rayleigh friction above the tropopause
C-1c	As for C-1a	0.00, -3.05, -20.32, -26.19, -28.13, 28.26, 34.91, 40.37, 45.10, 49.19, 52.05, 54.69, 56.20, 57.70, 58.31, 58.91, 59.26, 59.56, 59.76, 59.94	0.0, 0.0, 0.0, 0.0, 0.0, 0.0, 0.0, 0.0, 0.0, 0.0, 0.0, 0.0, 0.0, 0.0, 0.0, 0.0, 0.0, 0.0, 0.0, 0.5	Nonsymmetric forcing with a reversed meridional temperature gradient above the tropopause in the Southern Hemisphere

in the stratosphere, so that the model solution in this layer may resemble the weak stratospheric jet as observed in the first period (7–16 February 1990). Note, however, that, in absence of eddies, the thermal wind constraint is clearly broken in the stratosphere, at the price that a mean meridional circulation is established. One may think that this zonally symmetric circulation is confined to the stratosphere with a marginal influence in the troposphere because no internal dissipation is therein applied. It turns out that, in this case, the model supports a steady symmetric solution that peculiarly departs from the others already known. In the present paper it would be tempting to also assess the nature of this circulation. However, when the eddy field is included, the resulting zonally symmetric circulation departs greatly from this solution (see the appendix). Therefore, we decided to defer the detailed study of this symmetric solution to another occasion.

2) The second modification (C-1c) of the reference setup is obtained by introducing a nonsymmetric (with respect to the equator) thermal forcing in the stratosphere that leads to a reversed meridional temperature gradient in the Southern Hemisphere. Thus, a stratospheric thermally driven easterly zonal wind is possible. This forcing set up may crudely represent proper conditions for the summer hemisphere where the meridional ozone distribution may generate such a gradient in the stratosphere. In this case, as expected, the symmetric solution (no eddies)

follows the thermal wind constraint in the troposphere with a prevailing westerly jet decreasing/increasing above the thermal forcing tropopause in the Southern/Northern stratosphere (see the appendix).

For all three setups, the no-eddies solution is computed first by long time integrations to prove the effective role of the eddies in establishing and maintaining the double-jet structure in the troposphere in compliance with observations.

2) DIAGNOSTICS

We found that, disregarding the first year, the computed statistics remains stationary. Therefore, the experiments analyzed are run in perpetual conditions and the statistics are presented only for the seventh year (360 days). To illustrate the prominent features of the general circulation, a few diagnostic tools are available. Panels are selected for comparison with the case study: (i) the time-averaged zonal mean zonal wind, (ii) the E–P flux vectors with the associated divergence, (iii) the Eulerian mass streamfunction, and (iv) some Hovmoeller diagrams, which address the time variability of the zonal mean zonal wind anomaly and of the zonal mean eddy kinetic energy.

4. Tropospheric double-jet structure simulated: Effect of the stratosphere

Before discussing the solutions of the numerical experiments we note that, despite the different horizontal
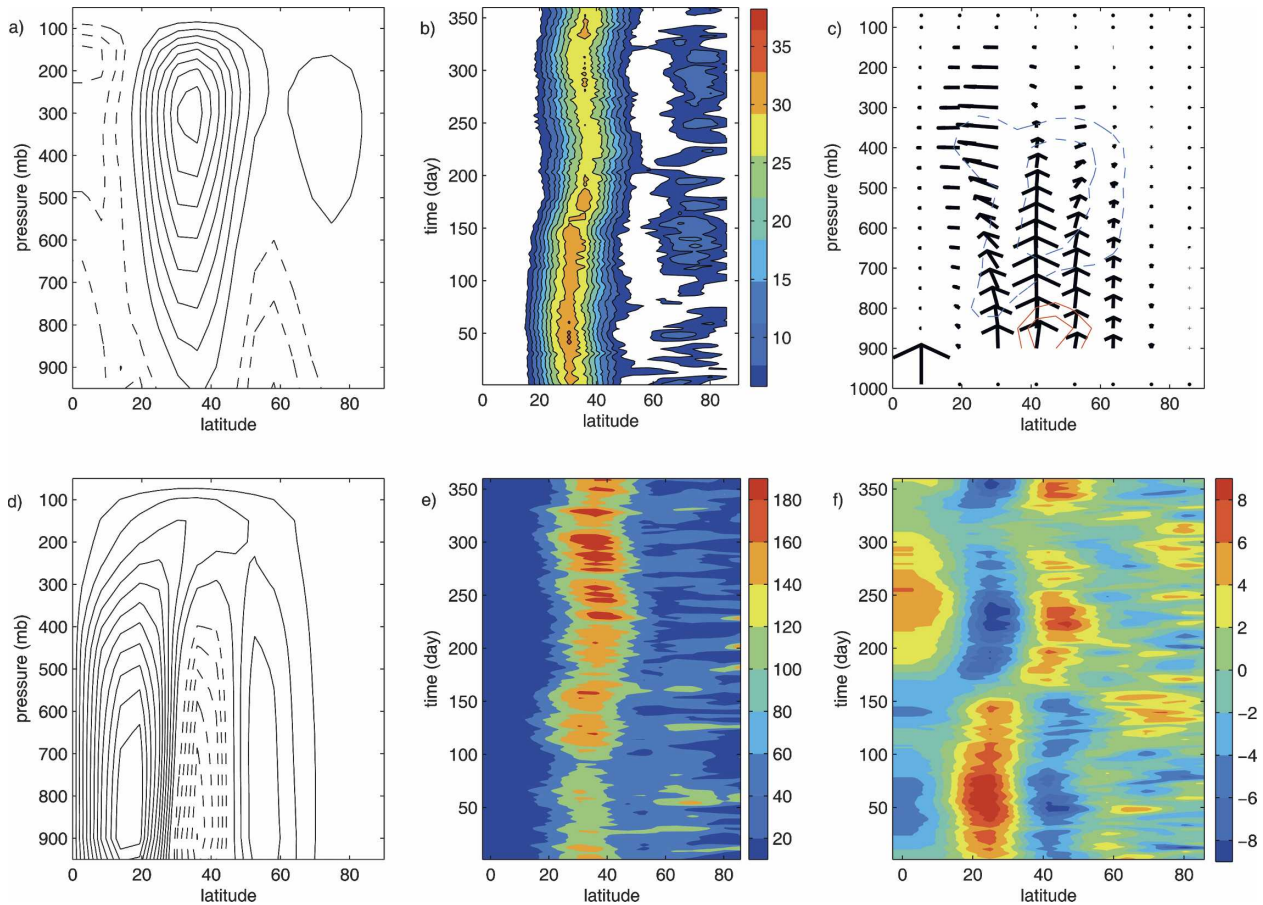
FIG. 4. Reference experiment (C-1a): (a) time-averaged (360 days) zonal mean zonal wind (m s^{-1}), (b) time evolution (Hovmoeller diagram) of the zonal mean zonal wind at 400 mb, (c) E–P flux (arrows) and the flux divergence field, (d) mass streamfunction ($\times 10^9$ kg s^{-1}), (e) zonal mean of the eddy kinetic energy at 500 mb (m^2 s^{-2}), and (f) time evolution (Hovmoeller diagram) of the zonal mean zonal wind anomaly at 500 mb (m s^{-1}). In (a) positive values (solid lines) are plotted every 4 m s^{-1}, while negative values (dashed lines) every 2 m s^{-1} and the zero line is omitted. In (c) units are the same as in Fig. 3. In (d) contours are every 4×10^9 kg s^{-1} with the zero line omitted.

and vertical resolution, we reproduce most of the results (not shown) obtained by Akahori and Yoden (1997) when the restoration temperature C-0 (Table 1) is considered.

a. Reference experiment (C-1a)

We obtain the following results. (i) The zonal mean zonal wind (Fig. 4a) shows a main westerly jet structure centered in the midlatitudes at 50°N, extending from the top of the model atmosphere down to the surface. It is sided by two secondary westerly upper-level jets located in the subtropical and polar regions, respectively. Their maximum intensities range from 1/3 to 1/9 of the midlatitude one and are located at different vertical levels. Lower-level easterlies are along these two secondary jets. (ii) The E–P vectors (Fig. 4c) indicate convergence of the eddy momentum flux toward these cen-

ters with a noticeable contribution coming from the eddy activity well above the tropopause forcing. The sign of the E–P flux divergence shows that the eddy field attempts to slow down the upper-level jets, while the low-level heat fluxes transport heat poleward. It appears that the E–P vector directions split around 50°N denoting a tendency to form a polar direct cell. (iii) The mass streamfunction supports this inference (Fig. 4d) revealing the classical three-cell picture. (iv) The vacillating nature of the two secondary jet maxima can be inferred from the time mean map and the Hovmoeller diagram (Fig. 4b) of the zonal mean zonal wind at 400 mb. For instance, around days 10–30, it is possible to distinguish two coexisting jets (see the main jet at about 50°N and the closed contour at about 25°N, Fig. 4b), while the polar one also shows an amplitude vacillation. The time scales of these vacillations are

FIG. 5. The C-1b setup: (a) time-averaged (360 days) zonal mean zonal wind, (b) time evolution (Hovmoeller diagram) of the zonal mean zonal wind at 400 mb, (c) E–P flux (arrows) and the flux divergence field, (d) mass streamfunction, (e) zonal mean of the eddy kinetic energy at 500 mb, and (f) time evolution (Hovmoeller diagram) of the zonal mean zonal wind anomaly at 500 mb. Units and contour intervals are the same as in Fig. 4.

long compared with the baroclinic cycle of the finite-amplitude eddy field (that is less than 10 days associated with a zonal wavenumber-7 structure; not shown). The zonal mean zonal wind anomaly at 500 mb (illustrated in Fig. 4f) resembles only partially the one discussed by James et al. (1994, their Fig. 5a), who noted a poleward propagation of the zonal wind anomaly. This propagation fails reaching the polar region, apparently due to the erratic vacillation of the main jet. When the midlatitude jet extends poleward, positive anomalies appear to propagate toward high latitudes (see the first 30 days or days 300–330). In other periods, instead, a tropospheric polar jet is formed when the lower-level easterlies at high latitudes penetrate deeply into the troposphere interrupting the poleward propagation of the zonal wind anomalies (see days 250–280). The zonal mean eddy kinetic energy (Fig. 4e) appears alternating in a quasi-regular manner at the latitude of the main jet, and periods of high values seem to be related to the strengthening of the midlatitude jet.

As observed, jet axis vacillations are of marginal importance. Overall, this experiment leads to the conclusion that the eddy field by itself may very well produce a general circulation consistent with the classical three-cell picture where a Hadley, Ferrel, and polar cell are present. On the other hand, we cannot neglect that observations firmly support a dominant winter hemisphere subtropical jet, whereas the model sets aside this feature for the midlatitude one. Moreover, these observations suggest the occurrence of easterlies in the summer stratosphere. In testing if our idealized model can comply with these observed features, we apply

- rayleigh friction above the tropopause (C-1b), and
- nonsymmetric radiative forcing above the tropopause [C-1c, see Eq. (6)].

b. Rayleigh friction above tropopause (C-1b)

The zonal wind (Figs. 5a,b) illustrates a considerable reduction of the stratospheric jet, while in the tropo-
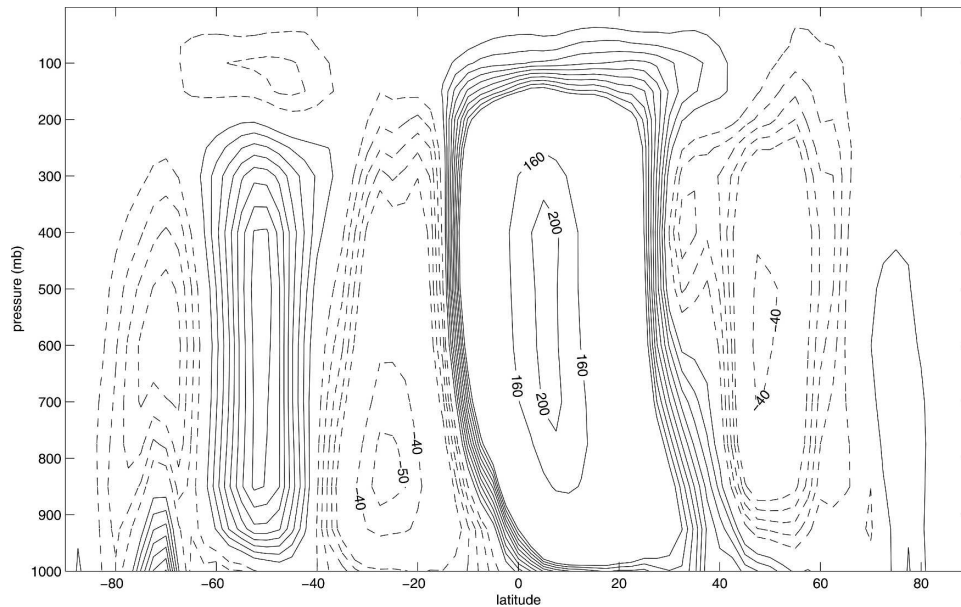
Fig. 6. Observations (February 1990): zonal mean cross section of the mass streamfunction for the monthly mean conditions ($\times 10^9$ kg s^{-1}). Contours are every 4×10^9 kg s^{-1} within the range (-20–40) and the zero line is excluded; values greater than 160×10^9 kg s^{-1} and less than -40×10^9 kg s^{-1} are labeled. Solid lines denote positive values, dashed lines denote negative ones.

sphere two jets coexist for a good portion of the time series. When the time mean flow is considered, they are located in the subtropics and in the mid- to high latitudes, consistently with the observed Northern Hemisphere circulation (Figs. 1a,b). The E–P vectors (Fig. 5c) split in the midlatitudes heading both toward the equator and the pole. The associated divergence shows a vertical dipole with negative contours uniformly distributed along the latitudes. This supports the mechanism leading to the jet vacillation as foreseen by Lorenz (1963): in polar regions the meridional wave axis is tilted westward, while in tropical regions it tilts eastward.

The mass streamfunction in Fig. 5d reveals a three-cell structure, but at upper levels the Hadley cell reaches the polar region through the stratosphere. Easterly vertical wind shear, in fact, is generated, inducing a thermally direct circulation below the level of the friction. This latter facet bears some similarities with the monthly averaged mass streamfunction of February 1990 in the Southern Hemisphere (Fig. 6), where a direct cell, above the Ferrel circulation, is clearly displayed (note that also in the Northern Hemisphere the mass streamlines of the Hadley cell tilt poleward at high levels, but they fail to reach polar region). The strong easterlies and dissipative processes (planetary wave breaking) in the Southern Hemisphere summer stratosphere might account for such feature of the general circulation.

The Hovmoeller diagram (Fig. 5b) of the zonal wind demonstrates a persistence of the two-jet structure. A long-period variability (amplitude and position) of the main jet is also noticeable and should be studied in more detail. However, such meridional wandering is not directly related to the main target of the paper (i.e., dynamics of the model at a synoptic time scale) and is just 10° or two grid points at our model resolution. Thus, in our view, this is not sufficient to study that behavior in detail and we leave further investigations to another occasion. The poleward propagation of the zonal wind anomaly is interrupted or slightly perceptible only at latitudes higher than 55°N (Fig. 5f). This is related to the vacillation of the two jet cores and the presence of easterlies between them. The eddy kinetic energy time series (Fig. 5e) decreases for long periods, in particular, when the subtropical jet reaches maximum values, as if the eddies were propagating in an effective background flow that does not allow a substantial growth of perturbations. By and large, the present case departs from James et al. (1994, their Fig. 5a) time mean and low-frequency behavior of the flow. Remarkably, despite the absence of any prescribed momentum and heat diffusion in the troposphere, the maximum jet intensity is located in the subtropics. This feature, as well as the number and the intensity of the tropospheric jets strongly depend on the external parameter choice, especially on the value of the Rayleigh friction at the surface, in agreement with the results by
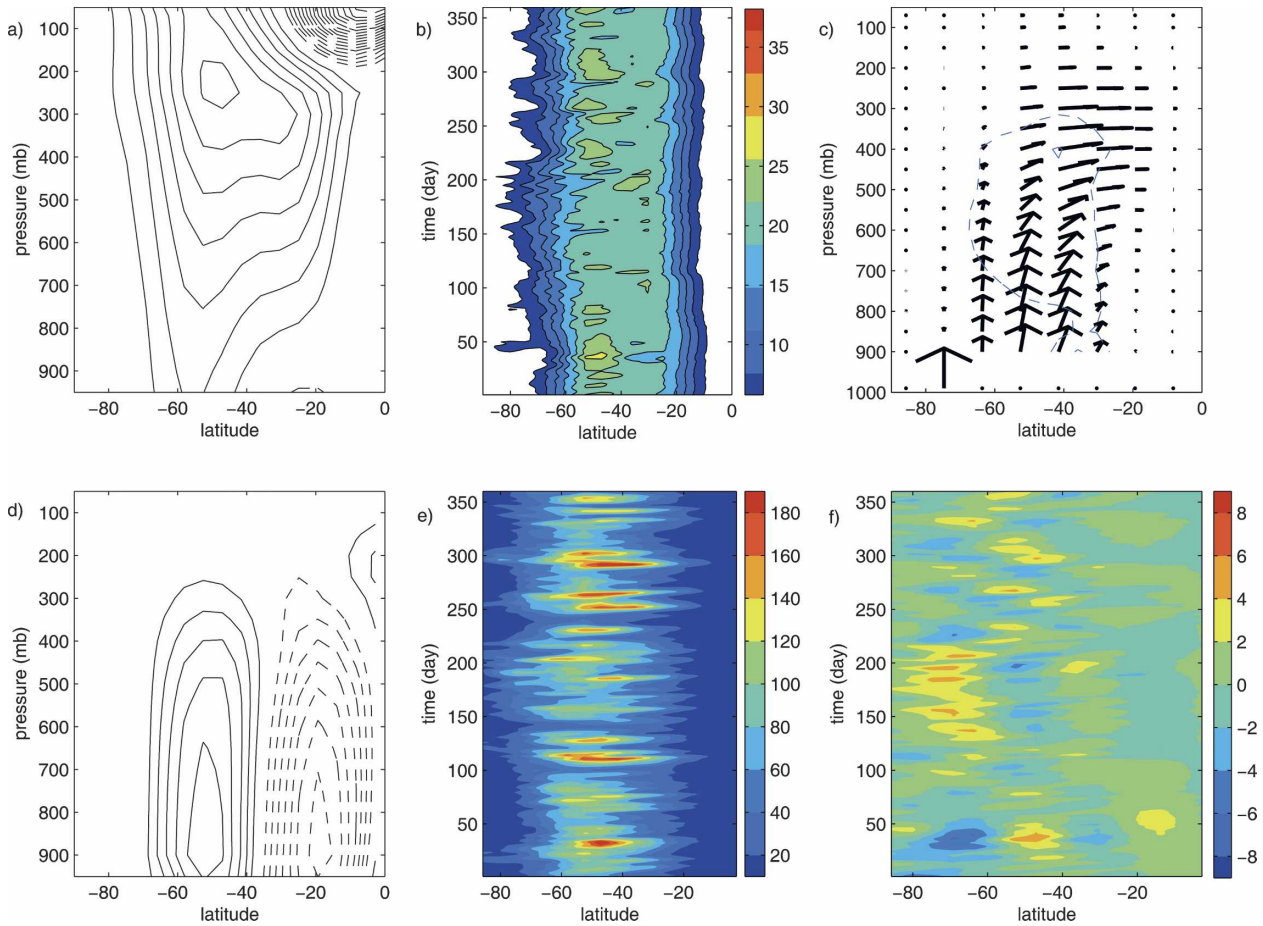
FIG. 7. The C-1c setup: (a) time-averaged (360 days) zonal mean zonal wind, (b) time evolution (Hovmoeller diagram) of the zonal mean zonal wind at 400 mb, (c) E–P flux (arrows) and the flux divergence field, (d) mass streamfunction, (e) zonal mean of the eddy kinetic energy at 500 mb, and (f) time evolution (Hovmoeller diagram) of the zonal mean zonal wind anomaly at 500 mb. Units and contour intervals are the same as in Fig. 4.

Robinson (1997) and Chen et al. (2007). We did not investigate this sensitivity as our aim is to show the formation of multiple jets as a function of the stratospheric forcing, leaving the set up of Akahori and Yoden (1997) unchanged for the troposphere.

c. Nonsymmetric radiative forcing above tropopause (C-1c)

The time mean statistics are summarized in Fig. 7 for the reversed meridional temperature gradient above the Southern Hemisphere tropopause. Note that the main jet axis (Fig. 7a) is in midlatitudes (cf. with the summer Southern Hemisphere observations, Fig. 1a) with a clear hint of a subtropical jet and easterlies in the upper tropical stratosphere. Moreover, Fig. 7b shows intermittent intensification of the subtropical jet. The E–P vectors (Fig. 7c) point equatorward for most of the hemisphere. Thus, stratospheric easterlies strongly

modify the zonal mean circulation forced by eddies that appear to propagate away from the source region toward the subtropics, depositing westerly momentum because of the absorption by equatorial easterlies. The mass streamfunction (Fig. 7d) shows weaker (with respect to the other cases) Hadley and Ferrel cells, and the former does not appear to be connected with the polar cell as it occurred in the previous run. More interestingly, the Hovmoeller diagrams of Figs. 7b,f suggest that the absence of the polar jet favors the poleward propagation of the zonal wind anomaly. The zonally averaged eddy kinetic energy (Fig. 7e) describes an aperiodic cycle with high intensity episodes corresponding to high values of the midlatitude jet. The overall picture appears to be consistent with the behavior of the Southern Hemisphere circulation observed in February 1990. However, at variance with these observations, the numerical solution does not show a direct cell topping the midlatitude Ferrel circulation. This feature

may easily be recovered by adding Rayleigh friction above the model tropopause. We refrain from seeking any further similarities since our goal is to illustrate the gross features of the general circulation.

5. Summary and conclusions

The role of the eddies in generating the main features of the observed low-frequency variability of the zonally averaged atmospheric circulation is analyzed. The first part of the paper illustrates the time variability of the observed zonally averaged zonal wind in a case study (a sample month of the ERA-40 reanalysis dataset): in the winter Northern Hemisphere, the analysis shows a period of several days characterized by a two-jet structure in the troposphere and another period during which a link between the midlatitude jet (weaker with respect to the other period) and the stratospheric polar jet occurs. The summer Southern Hemisphere is characterized by a strong tropospheric midlatitude jet, occasionally flanked by a subtropical one, and easterlies in the stratosphere. The second part of the work addresses the possible physical mechanisms leading to these observed features by means of a simplified general circulation model (i.e., PUMA). Different parameter settings and structures of the external radiative forcing in the stratosphere yield solutions of the model atmosphere consistent with the observed behavior. To isolate the effects of the eddies the same numerical experiments are performed without eddies (zonally symmetric solutions are illustrated in the appendix). Most of the observed features of the general circulation, including the occurrence of a secondary midlatitude jet alongside a strong subtropical one, are consistent with the baroclinic instability of the thermal wind solution. Furthermore, the following results emerge:

1) A weak stratospheric jet plays an important role in both the symmetric and the eddy response of the atmosphere to the thermal forcing; in particular, it appears to favor two coexisting tropospheric jets.

2) A weak stratospheric circulation may produce a Hadley cell that extends to the pole, overlying the Ferrel cell. The connection with the polar cell is achieved through the stratosphere. The few data presented here lend support to this peculiar feature, especially when the summer Southern Hemisphere is considered.

3) The radiative forcing with meridional temperature gradient reversal in the summer stratosphere may substantially contribute to some observed low-frequency variability of the circulation, as highlighted by the intermittent formation of the subtropical jet and the occurrence of easterlies in the tropical stratosphere.

4) The poleward propagation of the zonal wind anomaly often fails to reach polar regions in the first two cases presented, while it is more noticeable in the third case. The interruption of such propagation seems to be related to the variability pattern of the main tropospheric jet and the occasional occurrence of the polar jet. At variance with some observational studies, where the poleward propagation of the zonal wind anomaly is related to stationary waves, results suggest that synoptic eddies also contribute to such features of the zonal circulation (Feldstein 1998; Lorenz and Hartmann 2003).

Thus, it seems that the eddy dynamics alone may account for the observed meridional variance of the tropospheric jets even if impacts of other forcing have not been considered. The simplified general circulation model used here does not take into account some important aspects of the general circulation that may contribute to the magnitude and variability of the tropospheric jets. Just to mention a few, we have neglected sources of stationary forcing (e.g., land–sea contrast and orography) and any type of moist convection. Probably, if the land–sea contrast and orography were considered in the model, the longitudinal variability of the observed jets could be also represented. On the other hand, the impact of the moist convection should explain the different magnitude of the Hadley cell between observations and model runs. Furthermore, the statistical significance of the observed features is perhaps the least urgent question, while it appears more relevant to establish connections with other observed low-frequency variability patterns of the general circulation, such as the Artic Oscillation. Details on the eddy field affecting the radiative tropopause or the finite-amplitude baroclinic eddy structure should be studied.

Finally, model runs (shown in the paper), when compared with axisymmetric solutions (no eddies), reveal that the eddies also have a role in creating the subtropical jet. In addition, the streamlines cross the angular momentum contours near the poleward boundaries of the Hadley cell as suggested by Schneider (2006). However, we recognize that other effects neglected here, such as moist convection or tropical disturbances, may change the picture. We feel that, even if the angular momentum conservation is plausible to explain the genesis of the subtropical jet, further investigations should be done to clearly identify the role of synoptic eddies in creating the subtropical jet and the observed variability.

All the aspects mentioned above have been left for future works, because a complete assessment of them requires more than a single paper.
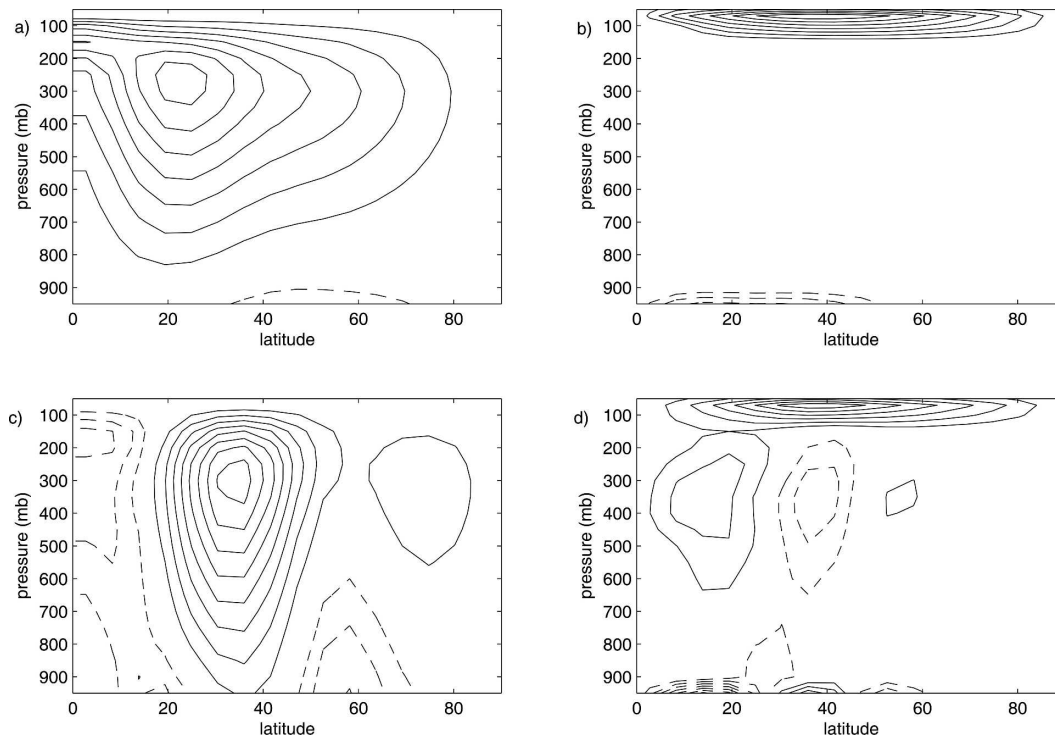
FIG. A1. Solutions for the C-1b setup: averaged zonal mean zonal and meridional wind (m s^{-1}) (a), (b) with no eddies and (c), (d) with eddies. In (a) and (c) positive values are plotted every 4 m s^{-1}, while negative values are plotted every 2 m s^{-1} and the zero line is excluded. In (b) and (d) values are plotted every 0.1 m s^{-1} and the zero line is omitted.

APPENDIX

Symmetric Solution with Rayleigh Friction above the Tropopause

In this appendix we will highlight the difference between the symmetric solutions obtained in the C-1b and C-1c setups and the ones that include eddies.

Note that Kuo (2001) studied a problem similar to that for C-1b setup with no eddies, but considering the case where Rayleigh friction is applied to all levels. He obtained substantially different results compared with ours. Thus, we can infer that our solution is entirely due to the particular vertical distribution of Rayleigh friction. As already stated, when we include Rayleigh friction in the upper stratosphere (see Table 1 for the details), a zonally symmetric solution exists in absence of the eddy field. The nature of this solution may be easily understood by inspecting the zonally averaged equations of motion. In fact, if we ideally divide the atmo-

sphere in two layers, namely a troposphere where the Rayleigh friction is acting only at the ground, and an upper layer wherein the Rayleigh friction acts everywhere, the mean meridional velocity must be nonzero in the troposphere because of the matching condition that must be satisfied at the interface between the two layers. It follows that a zonal mean flow, departing from the thermal wind balance, must be established with easterlies at the lower boundary. PUMA, starting from rest and in absence of eddies, after a long-lasting (more than 10 yr) transient, renders a steady axisymmetric solution as is shown in Figs. A1a,b, where the zonal and the meridional winds are sidewise plotted. Notice that the area covered by easterlies is far off the equator, while the jet maximum intensity is at about 20°N. There are unexpected features of this solution such as the westerly wind at the equator, with a secondary maximum above 200 mb. Moreover, westerlies extend well beyond the subtropics in most of the pressure columns. The mean meridional wind is essentially different from zero in the subtropics at the lower boundary, achieving its maximum intensity in the stratosphere at midlatitudes. As previously discussed, this solution is strongly modified by the eddy field. Actually, in the present case, eddies behave as it should be expected (Figs.
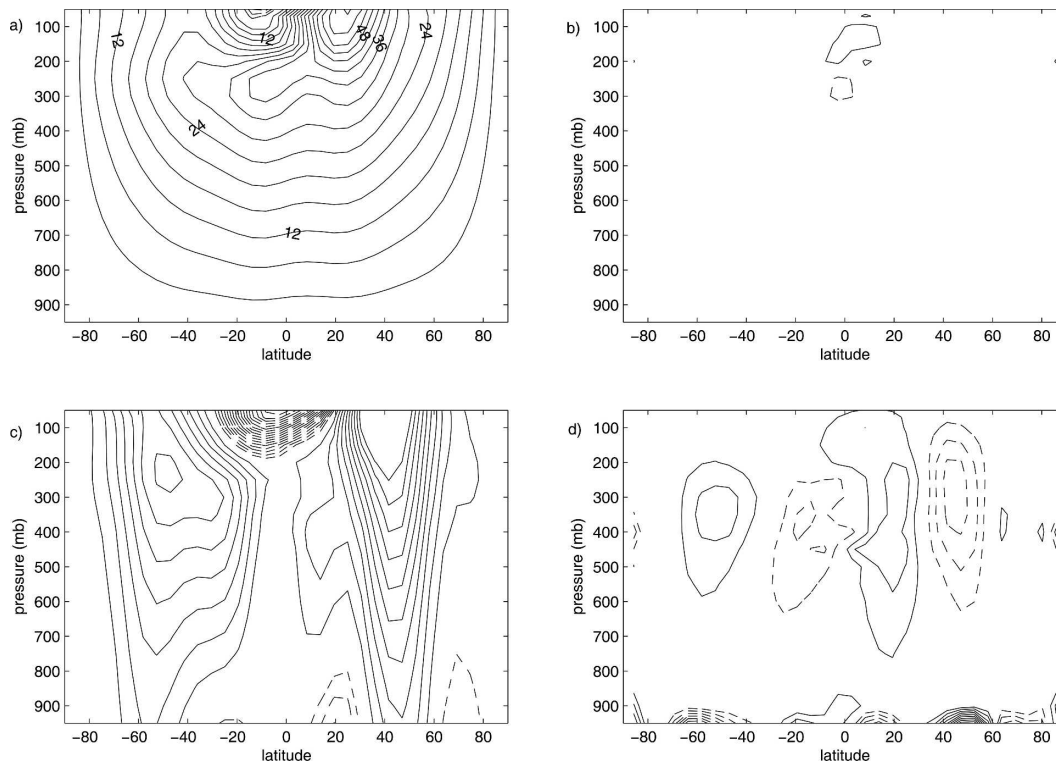
FIG. A2. Solutions for the C-1c setup: averaged zonal mean zonal and meridional wind (a), (b) with no eddies and (c), (d) with eddies. Units and contour intervals are the same as in Fig. 8.

A1c,d). The primary jet is moved poleward but it remains in the subtropics: easterlies are just at the most southern latitudes. Above all, the eddies considerably decelerate the mean meridional velocity in the stratosphere, creating a three-cell pattern in the upper troposphere of the model as it can be seen in Fig. A1d. This statistical steady state is reached shortly after we started the model from the symmetric solution or just from rest, but always allowing the eddy field to evolve freely.

The axisymmetric solution for C-1c setup is shown in Figs. A2a,b. As can be seen from these figures the no-eddy solution follows the thermal wind relation from the surface up to the forcing tropopause: a zonal mean zonal wind increasing with height with maximum values around the equator and no meridional velocity. In the stratosphere, instead, the solution is characterized by a prevalent westerly jet decreasing (increasing) with height in the Southern (Northern) Hemisphere and a weak meridional velocity around the equator. Because the no-eddy solution with a symmetric forcing and a reversed meridional temperature gradient in both hemispheres (not shown here) follows the thermal wind balance with a westerly jet decreasing above the thermal forcing tropopause, we may say that the particular

solutions of Figs. A2a,b are due to the nonsymmetric behavior of the forcing in the stratosphere. This kind of behavior is drastically modified by the action of the eddies as shown in Figs. A2c,d. In the Southern Hemisphere, a midlatitude jet at about 50°S occurs with a visible hint of a subtropical jet and easterlies in the upper tropical stratosphere. The Northern Hemisphere is characterized by a midlatitude jet extending up to the stratosphere and by hints of subtropical and polar jets. Finally, the meridional velocity clearly shows a two-cell pattern in the Southern Hemisphere and a three-cell structure in the Northern Hemisphere.

REFERENCES

Akahori, K., and S. Yoden, 1997: Zonal flow vacillation and bimodality of baroclinic eddy life cycles in a simple global circulation model. *J. Atmos. Sci.,* **54,** 2349–2361.

Bordi, I., A. Dell'Aquila, A. Speranza, and A. Sutera, 2002: Formula for a baroclinic adjustment theory of climate. *Tellus,* **54A,** 260–272.

——, ——, ——, and ——, 2004: On the midlatitude tropopause height and the orographic-baroclinic adjustment theory. *Tellus,* **56A,** 278–286.

Boville, B. A., 1984: The influence of the polar night jet on the tropospheric circulation in a GCM. *J. Atmos. Sci.,* **41,** 1132–1142.

Caballero, R., R. Castegini, and A. Sutera, 2001: Equilibration of a two-level primitive equation model on the sphere. *Nuovo Cimento,* **24,** 875–884.

Charney, J. G., 1959: On the theory of the general circulation of the atmosphere. *Rossby Memorial Volume,* B. Bolin, Ed., Rockefeller Institute Press, 178–193.

——, 1973: Planetary fluid dynamics. *Dynamic Meteorology,* P. Morel, Ed., D. Reidel Publishing Company, 97–351.

Chen, G., I. M. Held, and W. A. Robinson, 2007: Sensitivity of the latitude of the surface westerlies to surface friction. *J. Atmos. Sci.,* **64,** 2899–2915.

Dickinson, R. E., 1968: Planetary Rossby waves propagating vertically through weak westerly wind wave guides. *J. Atmos. Sci.,* **25,** 984–1002.

Edmon, H. J., Jr., B. J. Hoskins, and M. E. McIntyre, 1980: Eliassen-Palm cross sections for the troposphere. *J. Atmos. Sci.,* **37,** 2600–2616.

Eliassen, A., and E. Palm, 1961: On the transfer of energy in stationary mountain waves. *Geofys. Publ.,* **22** (3), 1–23.

Fang, M., and K. K. Tung, 1994: Solution to the Charney problem of viscous symmetric circulation. *J. Atmos. Sci.,* **51,** 1261–1272.

Feldstein, S. B., 1998: An observational study of the intraseasonal poleward propagation of zonal mean flow anomalies. *J. Atmos. Sci.,* **55,** 2516–2529.

Fraedrich, K., E. Kirk, and F. Lunkeit, 1998: Portable University Model of the Atmosphere. Deutsches Klimarechenzentrum, Rep. 16, 37 pp. [Available online at http://www.mi.uni-hamburg.de/puma.]

——, ——, U. Luksch, and F. Lunkeit, 2005: The Portable University Model of the Atmosphere (PUMA): Storm track dynamics and low frequency variability. *Meteor. Z.,* **14,** 735–745.

Frisius, T., F. Lunkeit, K. Fraedrich, and I. N. James, 1998: Storm track organization and variability in a simplified atmospheric circulation model. *Quart. J. Roy. Meteor. Soc.,* **124,** 119–143.

Hartmann, D. L., J. M. Wallace, V. Limpasuvan, D. W. J. Thompson, and J. R. Holton, 2000: Can ozone depletion and global warming interact to produce rapid climate change? *Proc. Natl. Acad. Sci. USA,* **97,** 1412–1417.

Held, I. M., 1975: Momentum transport by quasi-geostrophic eddies. *J. Atmos. Sci.,* **32,** 1494–1497.

——, and A. Y. Hou, 1980: Nonlinear axially symmetric circulations in a nearly inviscid atmosphere. *J. Atmos. Sci.,* **37,** 515–533.

——, and M. J. Suarez, 1994: A proposal for the intercomparison of the dynamical cores of atmospheric general circulation models. *Bull. Amer. Meteor. Soc.,* **75,** 1825–1830.

Hendon, H. H., and D. L. Hartmann, 1985: Variability in a nonlinear model of the atmosphere with zonally symmetric forcing. *J. Atmos. Sci.,* **42,** 2783–2797.

Hoskins, B. J., and A. J. Simmons, 1975: A multi-layer spectral model and the semi-implicit method. *Quart. J. Roy. Meteor. Soc.,* **101,** 637–655.

Hunt, B. G., 1978: Atmospheric vacillations in a general circulation model. Part II: Tropospheric-stratospheric coupling and stratospheric variability. *J. Atmos. Sci.,* **35,** 2052–2067.

James, I. N., and L. J. Gray, 1986: Concerning the effect of surface drag on the circulation of a planetary atmosphere. *Quart. J. Roy. Meteor. Soc.,* **112,** 1231–1250.

James, P. M., K. Fraedrich, and I. N. James, 1994: Wave-zonal-flow interaction and ultra-low-frequency variability in a sim-plified global circulation model. *Quart. J. Roy. Meteor. Soc.,* **120,** 1045–1067.

Koo, S., A. W. Robertson, and M. Ghil, 2002: Multiple regimes and low-frequency oscillations in the Southern Hemisphere's zonal-mean flow. *J. Geophys. Res.,* **107,** 4596, doi:10.1029/2001JD001353.

Kuo, H. L., 2001: On production of long-term mean zonal current and eddy momentum and heat transports in atmosphere. *Pure Appl. Geophys.,* **158,** 1047–1063.

Kushner, P. J., and L. M. Polvani, 2004: Stratosphere–troposphere coupling in a relatively simple AGCM: The role of the eddies. *J. Climate,* **17,** 629–639.

Lindzen, R. S., 1990: *Dynamics in Atmospheric Physics.* Cambridge University Press, 310 pp.

——, 1993: Baroclinic neutrality and the tropopause. *J. Atmos. Sci.,* **50,** 1148–1151.

Lorenz, D. J., and D. L. Hartmann, 2003: Eddy-zonal flow feedback in the Northern Hemisphere winter. *J. Climate,* **16,** 1212–1227.

Lorenz, E. N., 1963: The mechanics of vacillation. *J. Atmos. Sci.,* **20,** 448–465.

——, 1967: *The Nature and Theory of the General Circulation of the Atmosphere.* Meteor. Monogr., No. 218, World Meteorological Organization, 161 pp.

Matsuno, T., 1970: Vertical propagation of stationary waves in the winter Northern Hemisphere. *J. Atmos. Sci.,* **27,** 871–883.

Namias, J., 1950: The index cycle and its role in the general circulation. *J. Meteor.,* **7,** 130–139.

Norton, W. A., 2003: Sensitivity of northern hemisphere surface climate to simulation of the stratospheric polar vortex. *Geophys. Res. Lett.,* **30,** 1627, doi:10.1029/2003GL016958.

Palmén, E., 1949: Meridional circulations and the transfer of angular momentum in the atmosphere. *J. Meteor.,* **6,** 429–430.

Panetta, R. L., 1993: Zonal jets in wide baroclinically unstable regions: Persistence and scale selection. *J. Atmos. Sci.,* **50,** 2073–2106.

Peixoto, J. P., and A. H. Oort, 1992: *Physics of Climate.* Springer-Verlag, 520 pp.

Robinson, W. A., 1997: Dissipation dependence of the jet latitude. *J. Climate,* **10,** 176–182.

Rossby, C. G., and H. C. Willet, 1948: The circulation of the upper troposphere and lower stratosphere. *Science,* **108,** 643–652.

——, and V. P. Starr, 1949: Interpretations of the angular-momentum principle as applied to the general circulation of the atmosphere. *J. Meteor.,* **6,** 288.

Schneider, E. K., and R. S. Lindzen, 1977: Axially symmetric steady-state models of the basic state for instability and climate studies. Part I: Linearized calculations. *J. Atmos. Sci.,* **34,** 263–279.

Schneider, T., 2006: The general circulation of the atmosphere. *Annu. Rev. Earth Planet. Sci.,* **34,** 655–688.

Scott, R. K., and L. M. Polvani, 2004: Stratospheric control of upward wave flux near the tropopause. *Geophys. Res. Lett.,* **31,** L02115, doi:10.1029/2003GL017965.

Walker, C. C., and T. Schneider, 2006: Eddy influences on Hadley circulations: Simulations with an idealized GCM. *J. Atmos. Sci.,* **63,** 3333–3350.

Wittman, M. A. H., L. M. Polvani, R. K. Scott, and A. J. Charlton, 2004: Stratospheric influence on baroclinic lifecycles and its connection to the Artic Oscillation. *Geophys. Res. Lett.,* **31,** L16113, doi:10.1029/2004GL020503.